Effect of the Number of Arms on the Association of Amphiphilic Star Block Copolymers

Satu Strandman,[†] Anna Zarembo,[†] Anatoly A. Darinskii,[‡] Pasi Laurinmäki,[§] Sarah J. Butcher,[§] Elina Vuorimaa,[||] Helge Lemmetyinen,[||] and Heikki Tenhu*,[†]

Laboratory of Polymer Chemistry, University of Helsinki, Post Office Box 55, Helsinki, FIN-00014, Finland, Institute of Macromolecular Compounds, Bolshoi pr.31, 199004 St. Petersburg, Russia, Institute of Biotechnology and Department of Biological and Environmental Sciences, University of Helsinki, Post Office Box 65, Helsinki, FIN-00014, Finland, and Institute of Materials Chemistry, Tampere University of Technology, Post Office Box 541, Tampere, FIN-33101, Finland

Received July 2, 2008; Revised Manuscript Received September 16, 2008

ABSTRACT: Amphiphilic eight-arm star block copolymers with poly(methyl methacrylate) inner blocks and poly(acrylic acid) outer blocks were synthesized and their self-assembling properties were investigated in aqueous solutions. The critical aggregation concentrations of the stars were determined by steady-state fluorescence spectroscopy and static light scattering. The effects of salt, pH and the ionic strength on the self-assemblies have been investigated. Unlike in the earlier study on chemically similar four-arm stars, no transition in the morphology of aggregates was observed upon the addition of salt. The amphiphilic stars preferred forming spherical aggregates with low aggregation numbers at various solution conditions due to the steric crowding of the hydrophobic core as well as due to the remaining repulsion between the polyelectrolyte blocks in the outer shell. In addition to the experiments, computer simulations of the eight-arm amphiphilic star block copolymer with hydrophobic inner and hydrophilic outer blocks in a ratio 1:1 were studied using a coarse-grained model. It was observed that the eight-arm stars formed spherical micelle-like aggregates both in salt-free solutions and in the presence of salt, which is in agreement with the experimental results.

Introduction

The tailoring of polymers via controlled polymerization techniques has recently opened up new possibilities in the design and preparation of functional nanostructures based on supramolecular assembly. In aqueous solutions, a wide range of structures resembling those observed in nature can be obtained through self-assembling amphiphilic block copolymers, most commonly into spherical micelles, cylindrical micelles, and vesicles.[1] There has been growing interest toward investigating the principles of self-assembling and the stabilization of nanostructures because the potential applications as encapsulators or nanoreactors would require control of association behavior.[1,2] The self-assembling properties of amphiphilic block copolymers are dependent on the ratio of hydrophilic and hydrophobic blocks, as well as on properties of the solvent, like composition, pH, ionic strength, or the presence of organic additives.[3−5]

Brush-like or branched amphiphiles represent an interesting group of self-assembling polymers, as they may exist in aqueous solutions as single molecules having a core−shell structure, often called unimolecular micelles.[6,7] Among them are amphiphilic star block copolymers which, like their linear analogues, are capable of self-assembling into micelle-like aggregates.[8−10] In our recent papers, we have described the experimental findings and the simulations of the self-assembling properties of a four-armed starlike amphiphilic block copolymer, (PMMA-*b*-PAA)$_4$, with poly(methyl methacrylate) inner blocks and poly(acrylic acid) outer blocks in block length ratio 1:2 (PMMA/PAA).[11,12] The amphiphile formed spherical multimolecular micelles in a salt-free aqueous solution at pH ∼ 5. When salt was added, screening the charges of polyelectrolyte outer blocks induced the formation of cylindrical micelles,[11] which disintegrated again to spherical ones at high pH (pH ∼ 12) due to a higher degree of ionization and the swelling of the corona.[12] It has been observed earlier that the amphiphilic star polymers with different types of arms (heteroarm or miktoarm stars) are capable of forming micelle-like aggregates with cylindrical morphologies.[13,14] Similar behavior has also been observed for certain charged biopolymers like actin, which forms filamentous self-assemblies upon the addition of salt.[15]

Because the number of arms is expected to influence the interactions between the star polymers through the higher steric repulsion of the arms,[16,17] in the current work we have investigated the self-assembling characteristics of amphiphilic (PMMA-*b*-PAA)$_8$ star block copolymers with eight arms. Two copolymers with different ratios of hydrophobic PMMA inner blocks and hydrophilic PAA outer blocks have been synthesized, and their aggregation behavior has been probed in aqueous solutions by dynamic light scattering (DLS) and cryo-transmission electron microscopy both at low and high pH (pH ∼ 5 and pH ∼ 9). The aim has also been to explore whether changing the ionic strength of the solution would trigger the transition between various self-assembled morphologies in this sterically relatively hindered system. In addition to the experiments, the effect of salt on the self-assembling of an eight-arm amphiphilic star block copolymer has been investigated using coarse-grain computer simulations. This will be discussed in detail after describing the experimental findings on the self-assembling properties of the polymers.

Experimental Section

Materials. CuBr (99.999%), 4,4′-dinonyl-2,2′-bipyridine (dNbpy), *N*,*N*,*N*′,*N*″,*N*″-pentamethyldiethylenetriamine (PMDETA),

* To whom correspondence should be addressed. Tel.: +358919150334. Fax: +358919150330. E-mail: heikki.tenhu@helsinki.fi.
[†] Laboratory of Polymer Chemistry, University of Helsinki.
[‡] Institute of Macromolecular Compounds.
[§] Institute of Biotechnology and Department of Biological and Environmental Sciences, University of Helsinki.
[||] Tampere University of Technology.

10.1021/ma801475p CCC: $40.75
Published on Web 10/23/2008

and ethylene carbonate (EC, all from Aldrich), as well as trifluoroacetic acid (TFA, Riedel-de-Haën), were used without further purification. CuCl (Merck) was purified as described by Nikitine et al.[18] Anisole, *tert*-butyl acrylate, and methyl methacrylate (all from Aldrich) were distilled over CaH_2 prior to use. Dichloromethane (Fluka) and 1,4-dioxane (Merck) were dried on molecular sieves. Synthesis and characterization of octafunctional initiator, 4,6,10,12,16,18,22,24-octakis(2-bromoisobutyryl)-2,8,14,20-tetramethylresorcinarene, is reported elsewhere.[19] *N*,*N*,*N*′,*N*′,*N*′,*N*′-hexamethyl-1,2-ethanediaminium chloride (dimethonium chloride) was prepared by synthesizing the corresponding iodide salt, as described by McLaughlin et al.,[20] and exchanging the iodide counterions to chloride by Dowex 1 × 8−100 anion exchange resin (Acros Organics).

Syntheses of Star Polymers. *Synthesis of Starlike Poly(methyl methacrylate), (PMMA)$_8$.* A typical procedure was the following: Initiator (149 mg, 7.1×10^{-5} mol), 4,4′-dinonyl-2,2′-bipyridine (467 mg, 1.1 mmol), anisole (42.7 mL, 50% from the total volume of the reaction mixture), and methyl methacrylate (40.0 g, 399.5 mmol) were placed in a flask equipped with a high vacuum valve. The solution was degassed by two freeze−thaw cycles under high vacuum, after which CuCl (57 mg, 5.7×10^{-4} mol) was added, followed by three freeze−thaw cycles. The flask was placed in an oil bath thermostatted at 100 °C. After the reaction, the solution was cooled by dipping the flask into liquid nitrogen. The solution was brought to room temperature, after which the content was dissolved in THF and passed through a column packed with silica (4/5 of the total volume) and neutral alumina (1/5 of the total volume) in two layers to remove the copper salts. The polymer was precipitated in methanol and dried in vacuo at room temperature.

The conversion was determined by ^{1}H NMR from a sample of the reaction mixture in $CDCl_3$ by comparing the integrated areas of the signals of the monomer at 5.5 and 6.0 ppm (2H, vinyl group), as well as at 3.51 ppm (3H, $-CH_3$), with the signal of PMMA at 3.64 ppm (3H, $-CH_3$).[21] The number of arms (functionality, *f*) of the stars were calculated from integrated areas of the signals of the initiator at 6.60−5.26 (6H, Ar) and the signal of the end group at 3.76 (3H) by $f =$ 1H (end group)/1H (initiator), in which 1H stands for the integrated area of the signal corresponding to one proton.

The molar masses were calculated using the signal of PMMA at 3.60 ppm (3H, $-OCH_3$) by M_n (NMR) $= M_m \times f \times$ (1H (polymer)/1H (end group)) $+ M_i$, in which M_m and M_i are the molar masses of the monomer and the initiator, respectively. The overlapping area of the signals from the initiator (36H) was subtracted from the mutual area of PMMA (3H) and the end group (3H).

^{1}H NMR (200 MHz, $CDCl_3$) δ ppm: 7.17−5.26 (8H, Ar, initiator), 4.80−3.53 (36 H, initiator), 3.76 (3H, -OCH_3, end group), 3.60 (3H, -OCH_3), 1.89 and 1.46 (2H, -CH_2-), 1.40, 1.21, 1.02, and 0.84 (3H, -CH_3).

Synthesis of Star Block Copolymer of Poly(methyl methacrylate) and Poly(tert-butyl acrylate), (PMMA-b-PtBA)$_8$. A typical procedure was the following: Purified starlike $(PMMA)_8$ macroinitiator (1.5 g, 2.4×10^{-5} mol), with the molar mass of 63400 g/mol, and ethylene carbonate (3.26 g, 36.9 mmol, 16.8% from the mass of the monomer) were dissolved in *tert*-butyl acrylate (19.4 g, 0.15 mol, 22.2 mL) in a flask equipped with a high vacuum valve. PMDETA (40.8 μL, 32.8 mg, 0.19 mmol) was added to the solution and the solution was degassed by two freeze−thaw cycles. CuBr (27.4 mg, 0.19 mmol) was added, followed by three freeze−thaw cycles. The flask was placed in an oil bath thermostatted at 100 °C. After the reaction, the solution was cooled by immersing the flask into liquid nitrogen. The solution was brought to room temperature, after which the content was dissolved in THF and passed through a column packed with silica (4/5) and neutral alumina (1/5) in two layers. The polymer was precipitated in a mixture of methanol and water (8:2), washed with water, and lyophilized.

The conversion has been determined gravimetrically or by ^{1}H NMR from the sample of the reaction mixture in $CDCl_3$ by comparing the signals of the monomer at 5.4−6.7 ppm (3H, vinyl group) with the signal of PtBA at 2.17 ppm (1H, -CH-).[21] The molar mass of the block copolymer M_n (NMR) has been calculated using the block ratio determined by ^{1}H NMR and the molar mass of PMMA given by NMR.

^{1}H NMR (200 MHz, $CDCl_3$) δ ppm: 3.60 (3H, -OCH_3, PMMA), 2.22 (1H, -CH-, PtBA), 1.89 (2H, -CH_2-, PMMA), 1.81 (2H, -CH_2-, PtBA), 1.44 (9H, -C$(CH_3)_3$, PtBA), 1.02 and 0.84 (3H, -CH_3, PMMA).

Conversion of (PMMA-b-PtBA)$_8$ Star Block Copolymer to Amphiphilic (PMMA-b-PAA)$_8$. Hydrolysis of *tert*-butyl ester groups by trifluoroacetic acid in dichloromethane described by Ma and Wooley[22] was utilized to yield starlike $(PMMA\text{-}b\text{-}PAA)_8$. $(PMMA\text{-}b\text{-}PtBA)_8$ star block copolymer was dissolved in dry CH_2Cl_2, and the solution was flushed with nitrogen for 15 min. Trifluoroacetic acid (TFA, 5 equiv to the *tert*-butyl ester) was added and the mixture was stirred at room temperature for 24 h. The solvent and TFA were evaporated, and $(PMMA\text{-}b\text{-}PAA)_8$ polymer was dissolved in a mixture of water and acetone. The polymer was purified by dialyzing first in a water−acetone mixture (3:1) and then by gradually increasing the amount of water until the polymer was dialyzed against pure water. The polymer was dried by lyophilization.

To increase the degree of hydrolysis, a sample of amphiphilic polymer **1** was retreated with a large excess of trifluoroacetic acid (5 equiv to the *tert*-butyl ester groups of the unhydrolysed precursor) in a mixture CH_2Cl_2 and dry 1,4-dioxane (volume ratio 2:1). The solution was flushed with nitrogen for 15 min prior to the injection of TFA. The mixture was stirred at 30 °C in a dark environment for 2.5 h, after which the product was purified as above.

The ^{1}H NMR signal from the -CH- protons of poly(*tert*-butyl acrylate) at 2.18 ppm disappeared while that of poly(acrylic acid) appeared at 2.39 ppm upon the hydrolysis. No cleavage of the methyl ester groups of poly(methyl methacrylate) was observed. The degree of hydrolysis has been estimated from the integrated area of the remaining signal of *tert*-butyl ester protons at 1.37 ppm, which has been compared with the integrated areas of the signals of PAA after the subtraction of overlapping signals from PMMA and PtBA.

^{1}H NMR (200 MHz, DMSO-d_6) δ ppm: 3.55 (3H, -OCH_3, PMMA), 2.20 (2H, -CH-, PAA and PtBA), 1.73 and 1.50 (6H, -CH_2-, PMMA, PtBA and PAA), 1.37 (9H, -C$(CH_3)_3$, PtBA), 0.93 and 0.76 (3H, -CH_3, PMMA).

Methods. *Nuclear Magnetic Resonance Spectroscopy (NMR) and Size Exclusion Chromatography (SEC).* NMR spectra were measured with a 200 MHz Varian Gemini 2000 NMR spectrometer (operating at 200 MHz for ^{1}H). The chemical shifts are presented in part per million using the solvent signal as a reference. The SEC analyses, giving molar masses and molar mass distributions, were performed with a Waters instrument equipped with Styragel guard column, 7.8 × 300 mm Styragel capillary column, and Viskotek 270 Dual Detector connected with the Waters 2487 UV and Waters 2410 RI detectors. THF was used as an eluent with a flow rate 0.8 mL/min. The calibrations were performed with poly(methyl methacrylate) standards from Polymer Standards Service GmbH.

pH Measurements and Potentiometric Titrations. The pH measurements and the potentiometric titrations of the amphiphilic star block copolymers were performed using a PHM210 standard pH meter (Meterlab, Radiometer, Copenhagen), which was calibrated prior to each series of measurements or each titration with pH buffer standards 4.0 and 10.0 (Merck) at 22 °C. Solutions (5.0 g/L) of the polymers in aqueous 0.1 M NaCl at pH 11.5 were titrated by 0.1 M aqueous HCl containing 0.1 M NaCl. The titrations were performed from pH 11.5 to pH 2.0, allowing 2 min equilibrium time between each point. The equivalence points of the titrations were set as the points of intersection of the inflection tangents of the curve. The degrees of dissociation, α, and the apparent values of pK_a (pH at which $\alpha = 0.50$) were determined from the titration curve (data presented in the Supporting Information).

Steady-State Fluorescence Spectroscopy. The polymers were solubilized in water by a small addition of 5.0 M NaOH solution

to give 5.0 g/L stock solutions with pH ~ 5.2, which were used for successive dilutions down to 1.22×10^{-9} g/L. The probe, 4-(dicyanomethylene)-2-methyl-6-(*p*-dimethylaminostyryl)-4*H*-pyran (4HP), was dissolved in chloroform. A series of samples was prepared by injecting 100 μL of 0.1 mM probe solution to an empty vial, evaporating the chloroform by flushing with nitrogen at room temperature, and adding 3 mL of the polymer solution to the vial yielding the probe concentration of 3.33×10^{-6} M. The samples were sonicated for 10 min and kept overnight at 40 °C. Fluorescence spectra were recorded using Spex Fluorolog 3 spectrofluorometer (right-angle geometry, 1 × 1 cm quartz cell) using the following conditions: excitation at 432 nm, recording range 480−800 nm, slit width 3 nm for the excitation and 3 nm for the emission. Absorption spectra were recorded by UV-3600 Shimadzu UV−vis-NIR spectrophotometer (1 × 1 cm quartz cell).

Light Scattering. Deionized water (purified by ELGA PURELAB Ultra system) was used in preparation of all solutions. The solutions were prepared by direct dissolution of the powderlike lyophilized amphiphilic star block copolymers in water at room temperature to give 5.0 g/L stock solutions. The pH of the solutions was adjusted either to pH ~ 5 or to pH ~ 9 to solubilize the polymer by adding small amounts of 5.0 M NaOH, after which the solutions were equilibrated for several days at room temperature prior to the addition of salt. Salt solutions for light scattering and cryoTEM were prepared by the addition of concentrated NaCl (5.0 M) solution to a known volume of 5.0 g/L aqueous polymer solution until the concentration of NaCl was 0.1−0.4 M.

Static light scattering (SLS) and DLS measurements were conducted with a Brookhaven Instruments BI-200SM goniometer and a BI-9000AT digital correlator. Ar-pumped laser (LEXEL 85, $\lambda = 488.0$ nm) or a solid-state laser (Coherent Sapphire, $\lambda = 488.0$ nm) was used as a light source. In DLS the time autocorrelation function of scattered light intensity

$$G_2(t) = \langle I(0)I(t)\rangle \quad (1)$$

was collected in self-beating mode. The correlation functions were analyzed by the inverse Laplace transform program CONTIN to obtain distributions of relaxation times, τ, of corresponding correlation functions of electric field, G_1(t), distributions of relaxation rates, $\Gamma = \tau^{-1}$, or distributions of hydrodynamic radii, R_h. The values of the refractive index and the viscosity of water were used for aqueous solutions. The temperature was 20 °C and the range of the studied scattering angles was 40−150°. The equipment was calibrated using toluene.

The radii of gyration, R_g, corresponding to the fast and slow relaxation processes of the bimodal relaxation time distribution were determined by calculating the relative amplitudes of the relaxation processes extracted from the amplitude of the total intensity of scattered light $A_i(\tau_i)$ using the procedure outlined by Klucker et al.[23]

$$A_f \equiv \sum_{\text{fast}} A_i(\tau_i) \quad \text{and} \quad A_s \equiv 1 - A_f \quad (2)$$

where $A_f(q)$ and $A_s(q)$ are the relative amplitudes of the fast and slow relaxation processes, respectively. The relative amplitudes $A_f(q)$ and $A_s(q)$ were converted into the time-averaged intensities associated with the relaxation processes, $I_f(q)$ and $I_s(q)$

$$I_f = A_f(q) \cdot I(q) \quad \text{and} \quad I_s = A_s(q) \cdot I(q) \quad (3)$$

The values of R_g were obtained from the slope of the reciprocal intensities versus q^2 (see Supporting Information for an example).

Cryo-electron Microscopy. Aliquots (3 μL) of the investigated polymers in aqueous solutions at 5.0 g/L were pipetted onto 400 mesh copper grids covered with a holey carbon film (Quantifoil R 2/2) and vitrified by plunging into liquid ethane.[24] Samples were maintained at −180 °C in a Gatan 626 cryoholder, while images were recorded on an FEI Tecnai F20 field emission gun transmission electron microscope (Electron Microscopy Unit, Institute of Biotechnology, University of Helsinki) at 200 kV under low-dose conditions at a nominal magnification of 50000× on Kodak SO163 film or at 68000× on a Gatan UltraScan 4000 CCD camera. Micrographs that were free of drift and astigmatism were digitized at 7 μm intervals on a Zeiss Photoscan TD scanner resulting in a nominal sampling of 1.4 Å pixel^{-1}. The sampling of the digital images obtained on the CCD camera was 2.21 Å pixel^{-1}.

Scheme 1. Structure of the Octafunctional Initiator

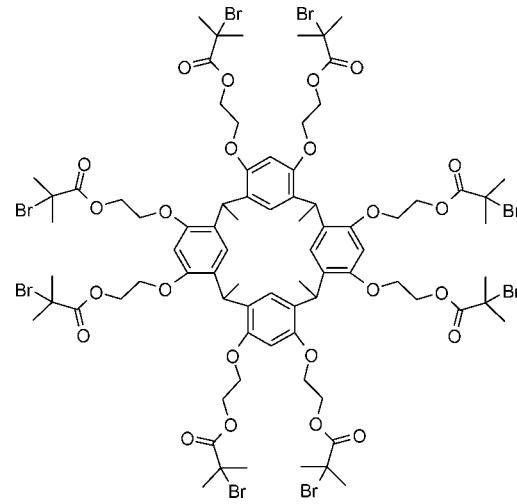

Results and Discussion

Synthesis of (PMMA-*b*-PAA)$_8$ Star Block Copolymers. Amphiphilic star block copolymers with eight arms were synthesized stepwise using an octafunctional initiator by the block copolymerization of methyl methacrylate, MMA, and *tert*-butyl acrylate, tBA, by the atom transfer radical polymerization (ATRP) method, followed by the hydrolysis of *tert*-butyl ester groups. The aim has been to prepare eight-armed stars with similar composition as in our earlier study[11] on a four-armed amphiphilic star (PMMA$_{73}$-*b*-PAA$_{143}$)$_4$ but with two different ratios of the blocks. In the first step, starlike poly(methyl methacrylate), (PMMA)$_8$, macroinitiator was synthesized using an octafunctional resorcinarene-based initiator bearing a spacer between the macrocycle and the initiating group (Scheme 1).[19] The visible signals from the initiator allowed the determination of the numbers of arms (as denoted herein as functionality *f*) by ^{1}H NMR, which were close to eight (Table 1). Purified (PMMA)$_8$ was then used in the block copolymerization of *tert*-butyl acrylate. Both polymerizations of MMA and tBA were stopped at low conversion to avoid bimolecular coupling reactions. However, the size exclusion chromatograms of star block copolymers given by a light scattering detector (Figure 1) showed two peaks, of which the shoulder at higher molar masses corresponds to the star−star coupled product (intermolecular coupling), and its area is 10% of the total area of peaks for both of the investigated star block copolymers. Because the light scattering detector emphasizes large scatterers and the peak of the coupled product was not visible in the chromatograms by RI detector (data not shown here), we may expect that the amount of the coupled stars is very low.

In the final step, amphiphilic (PMMA-*b*-PAA)$_8$ stars were obtained by the acidic hydrolysis of poly(*tert*-butyl acrylate) to poly(acrylic acid) with trifluoroacetic acid. According to ^{1}H NMR in DMSO-d_6 and in D_2O/$CDCl_3$, the degrees of hydrolysis for polymers **1** and **2** were 89 and 95%, respectively. To estimate how the higher hydrophobic/hydrophilic ratio affects the solution properties of polymer **1**, a second hydrolysis was carried out on a sample of amphiphilic polymer **1**, which increased the degree of hydrolysis to 95%. The amphiphilicity of the stars was demonstrated by ^{1}H NMR by adding some $CDCl_3$ to the

Table 1. Properties of the Synthesized Star Polymers[a,b]

entry	polymer	[*M*]/[*I*]	*t*, min	conv %	M_n(theo),[a] g/mol	M_n(NMR),[b] g/mol	M_n(SEC, RI) g/mol	M_w/M_n (RI)	M_n(SEC, LS),[b] g/mol	M_w/M_n (LS)	*f* (NMR)
1	$(PMMA)_8$	5600	20	9.1	53100	63500	50500	1.15	63400	1.20	8
	$(PMMA\text{-}b\text{-}PtBA)_8$	6400	50	11.7	159100	151400	114700	1.13	134500	1.17	
	$(PMMA\text{-}b\text{-}PAA)_8$					117200(112900)			106900(103500)	1.17	
2	$(PMMA)_8$	5600	20	8.6	50300	54000	50100	1.13	53900	1.17	7.7
	$(PMMA\text{-}b\text{-}PtBA)_8$	6400	75	14.0	168800	164700	133400	1.18	142500	1.28	
	$(PMMA\text{-}b\text{-}PAA)_8$					118700(116200)			105700(103700)	1.28	

[a] M_n(theo) = (conversion × [*M*]/[*I*] × M_m) + M_i, where M_m and M_i are molar masses of the monomer and initiator, respectively. [b] The molar masses of the amphiphiles have been calculated using the degrees of hydrolysis of the *tert*-butyl groups given by ^{1}H NMR in DMSO-d_6 for polymers **1** and **2**, being 89 and 95%, respectively. The molar masses calculated using 100% degree of hydrolysis of the *tert*-butyl groups are given in parentheses.

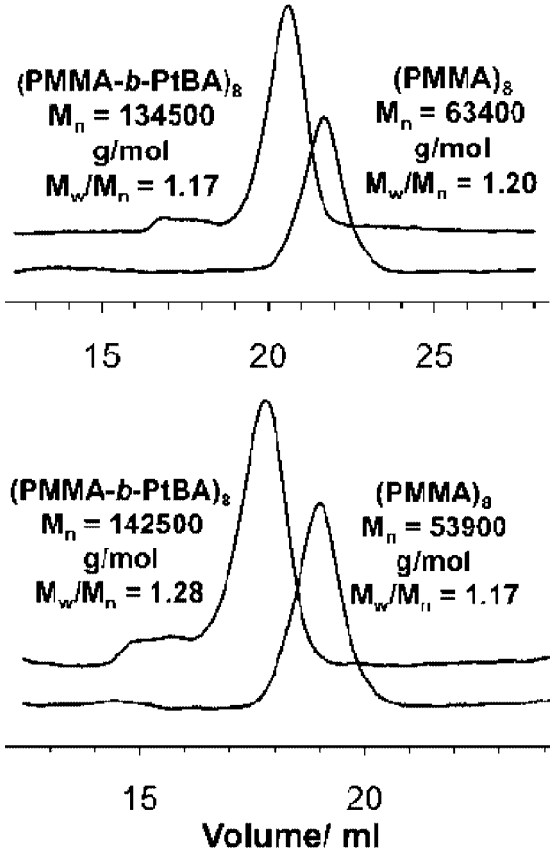

Figure 1. SEC traces of starlike $(PMMA)_8$ and the corresponding block copolymer $(PMMA\text{-}b\text{-}PtBA)_8$ by light scattering detector for entries **1** and **2** in Table 1.

samples in D_2O. This made the resonance signals of PMMA appear upon the increased mobility of the core inside the PAA shell. In D_2O, all the signals of PMMA were invisible. The properties of the star polymers are presented in Table 1. The compositions of the amphiphiles have been calculated from the block ratios given by ^{1}H NMR and the values of M_n (NMR) for $(PMMA\text{-}b\text{-}PtBA)_8$ precursors, being $(PMMA_{77}\text{-}b\text{-}PAA_{86})_8$ for the polymer **1** (ratio of the degrees of polymerization PMMA/PAA = 1:1.1) and $(PMMA_{65}\text{-}b\text{-}PAA_{108})_8$ for the polymer **2** (ratio of the degrees of polymerization 1:1.7).

The amphiphilic star block copolymers were not soluble in water below pH 4.70 (degree of dissociation $\alpha < 0.10$) owing to the poor solubility of protonated poly(acrylic acid) outer blocks but required a small addition of NaOH to dissolve at pH 4.80. Therefore, we investigated the effect of pH on the degree of ionization by potentiometric titration of the polymer solutions (5.0 g/L; presented in the Supporting Information). The apparent values of pK_a were 5.70 for both amphiphiles, being in the same range as the ones reported for linear block copolymers of poly(*n*-butyl acrylate) and poly(acrylic acid) (pK_a = 5.50−5.70) as well as for linear poly(acrylic acid) (pK_a = 5.40), both in 0.1 M NaCl.[25,26] The similarity between the two amphiphiles arises from the minor difference in the lengths of poly(acrylic acid) blocks. Unless mentioned otherwise, the results below have been obtained at average pH 5.25 ± 0.15 corresponding to $\alpha = 0.25 \pm 0.07$ for polymer **1** and $\alpha = 0.25 \pm 0.06$ for polymer **2**.

Critical Aggregation Concentration (cac) of the Amphiphilic Stars. Amphiphilic star block copolymers with low number of arms ($f = 3$ or 4) are well-known to self-assemble to micelle-like aggregates in aqueous solutions.[11] The same behavior has also been observed for stars with higher functionalities ($f \geq 6$),[27,28] being in agreement with the simulations.[16,29] The onset of micelle formation of amphiphilic polymers has often been determined by the steady-state fluorescence spectroscopy of pyrene, utilizing the ratio of the intensities of the first (I_1) and the third (I_3) vibrational bands of the emission spectrum of pyrene, sensitive to the polarity of the immediate environment of the probe.[30] However, the use of pyrene turned out to be difficult in our case for the determination of cac, as the core of the amphiphilic stars, resorcinarene, has its fluorescence emission maximum at $\lambda_{em} = 338$ nm (excitation wavelength $\lambda_{excit} = 281$ nm) and the band is partially overlapping those of pyrene. Therefore, it was necessary to choose another probe with the emission spectrum at higher wavelengths.

4-(Dicyanomethylene)-2-methyl-6-(*p*-dimethylaminostyryl)-4*H*-pyran (4HP) is a fluorescence probe that is solubilized within the hydrophobic domains. 4HP contains both electron donor and acceptor moieties linked by an aromatic chromophore, and because both twisting about the double bond and a charge separation are involved in the formation of intermolecular charge transfer (ICT) states, its fluorescence emission is sensitive both to the polarity of the solvent and to the microviscosity of the medium. It has been used for investigating proteins, micelles and aggregates, as well as for monitoring the lower critical solution temperature (LCST) characteristics of a thermosensitive polymer.[31−34]

We used the steady-state fluorescence spectroscopy of 4HP to determine the onset of aggregate formation of the amphiphilic stars. 4HP has been reported to exhibit a band with emission maximum at $\lambda_{em} = 530$ nm in a nonpolar medium, such as *n*-heptane. Increasing the solvent polarity induces a red shift in the emission maximum, for instance, to $\lambda_{em} = 620$ nm in methanol.[31] At low polymer concentrations below the onset of micellization, the emission maximum of 4HP was at $\lambda_{em} = 647$ nm ($\lambda_{excit} = 432$ nm, absorption wavelength $\lambda_{abs} = 435$ nm), indicating the highly polar environment of the probe. A Raman scattering band arising from the vibrational and rotational transitions of water was clearly distinguishable at low polymer concentrations at $\lambda_{em} = 506$ nm. When the polymer concentration was increased, the emission maximum blue-shifted above the onset of micellization to $\lambda_{em} = 585$ nm for polymer **1** and to $\lambda_{em} = 590$ nm for polymer **2** ($\lambda_{abs} = 463$ and 460 nm, respectively) reflecting a less polar environment for the probe within the micellar core. Both of the values are higher than reported in the literature[35] for 4HP in solid PMMA, $\lambda_{em} = 550$

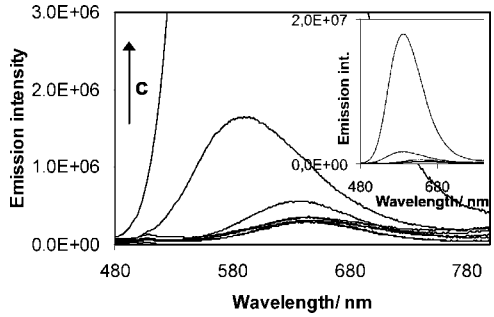

Figure 2. Fluorescence emission intensity of 4HP (3.33×10^{-6} M) as a function polymer concentration, c, for the amphiphilic star polymer **2** (PMMA/PAA = 1:1.7) at the range 1.22×10^{-9} to 1.22×10^{-1} g/L. The inset represents the same spectra, now showing the full peak at the highest polymer concentration.

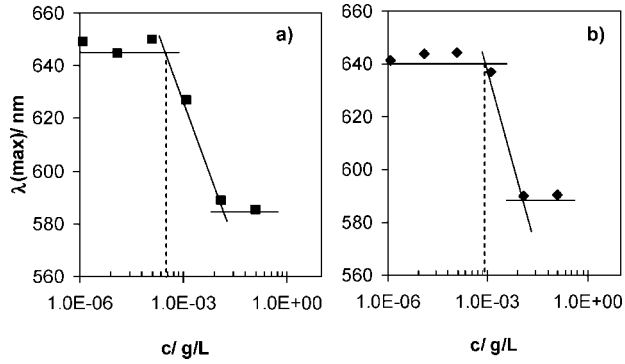

Figure 3. Determination of critical aggregation concentration, cac, using fluorescence emission maxima of 4HP in aqueous solutions of the amphiphilic star polymers **1** (a) and **2** (b) as a function of polymer concentration.

nm (λ_{excit} = 420 nm, λ_{abs} = 453 nm), indicating a low density of the hydrophobic core. The difference between the emission maxima of the two polymers could originate from the different packing densities of the starlike amphiphiles in micelles or rather from the slower diffusion of the probe within the hydrophobic core surrounded by longer polyelectrolyte chains (polymer **2**). The blue shift was accompanied by an increase in emission intensity, as shown by Figure 2, suggesting changes in microviscosity in the vicinity of the probe upon the micellization of the polymers.

The cac was determined as the intersection between the plateau in the emission maximum at $\lambda_{em} \sim 647$ nm and the tangent of the decreasing λ_{em} as a function of polymer concentration (Figure 3). The cac was $(0.35 \pm 0.04) \times 10^{-3}$ g/L for polymer **1** and $(0.90 \pm 0.05) \times 10^{-3}$ g/L for polymer **2**, and the cac values determined as the onset of increasing light scattering intensities (data presented in the Supporting Information) were $(0.80 \pm 0.21) \times 10^{-3}$ g/L and $(1.80 \pm 0.44) \times 10^{-3}$ g/L, respectively. All results were determined in the absence of salt. The effect of salt was not studied due to poor solubility of the probe in saline solutions. The cac is, as expected, lower for polymer **1**, which has a slightly longer hydrophobic block and a higher fraction of the hydrophobe. The remaining *tert*-butyl ester groups of polymer **1** (11%) had only minor effect on the cac, as the light scattering measurements of the further hydrolyzed sample of **1** (5% *tert*-butyl ester groups) gave a cac $(0.85 \pm 0.26) \times 10^{-3}$ g/L. This value is within the error of the sample with lower degree of hydrolysis. The reason for the different values given by the two methods may lie in the uncertainties in determining the intersection in the fluorescence data or the exact point at which the light scattering intensity starts to increase. Another explanation could stem from the

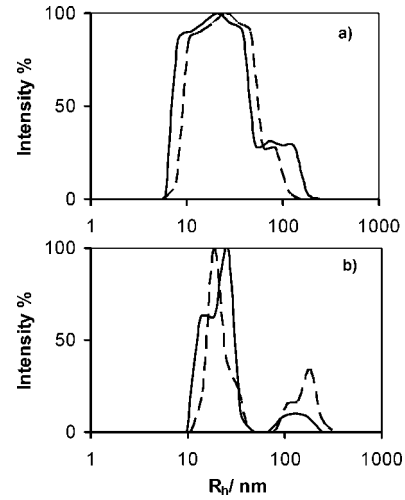

Figure 4. Distributions of hydrodynamic radius obtained at 90° scattering angle for 5.0 g/L solutions of amphiphilic star polymers **1** (a) and **2** (b) in aqueous NaCl. Dashed line represents ionic strength I = 0.10 M and solid line I = 0.36 M.

principles of the methods: light scattering is a noninvasive method that requires no external probe, while fluorescence spectroscopy utilizes a hydrophobic probe, which may perturb the hydrophobic interactions in the studied system despite its low concentration. Nevertheless, the obtained values of cac give an idea of concentrations below which the amphiphiles are expected to exist as unimolecular micelles in salt-free solution. The values are similar to the ones reported by Kim et al.[9] for three- and four-armed poly(ε-caprolactone)-*block*-poly(ethylene glycol) stars with block ratios 1:1 (cac determined by fluorescence spectroscopy, being 1.40×10^{-3} and 0.80×10^{-3} g/L, respectively).

Properties of the Aggregates. The characteristics of the aggregates were studied by DLS and cryo-transmission electron microscopy (cryoTEM) above the cac at constant polymer concentration, 5.0 g/L, but varying the pH and ionic strength of the solutions. Most of the measurements have been conducted at low pH (pH 5.10) to compare the morphologies of the aggregates with those reported earlier for the four-arm star block copolymers of PMMA and PAA.[11] At low pH, the polymers precipitated when the ionic strength of saline solutions reached 0.4 M, while at high pH (pH ~ 9) they tolerated even higher NaCl concentrations. When divalent salts like $CaCl_2$ or dimethonium chloride were added, the bridging between the polyelectrolyte chains led to precipitation at significantly lower salt concentrations (≤15.0 mM) compared to the monovalent salts. The effect of divalent salts on the aggregation behavior will not be discussed here. In general, polymer **2** was less prone to precipitation due to its higher hydrophilicity.

All the investigated samples gave bimodal size distributions by DLS both at 90° and 40° measuring angles (examples shown in Figure 4). Some reasons for bimodal size distributions are intermolecular interactions (due to aggregation, too high polymer concentration, or the polyelectrolyte effect) or the coexistence of both rotational and translational diffusion processes typical for the nonspherical species.[36,37] CryoTEM micrographs of the samples showed two populations of particles with different sizes. Polydispersity of the samples may cause deviation from a single exponential decay of correlation functions. The value $p = \mu_2\Gamma^2$ obtained from the second-order cumulant fit (polynomial fit of the second order), where μ_2 is the second cumulant and $\Gamma = \tau^{-1}$ is the decay rate, often called the first cumulant, has commonly been used as a measure of the polydispersity of the decay rate distribution.[38] Therefore, the second-order cumulant analysis was not appropriate for the correlation functions

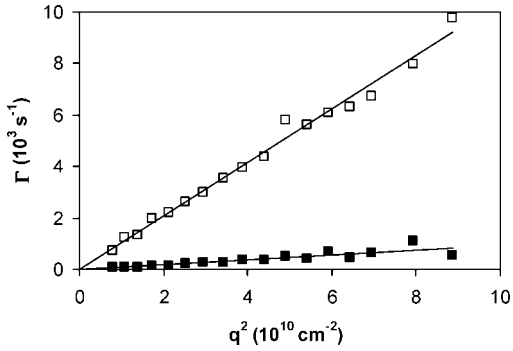

Figure 5. Mean relaxation rates Γ as the function of the squared amplitude of the scattering vector q^2 for 5.0 g/L solution of the amphiphilic star polymer **2** in aqueous 0.36 M NaCl. Open symbols correspond to the fast diffusion mode (low R_h) and solid ones to the slow diffusion mode (high R_h).

deviating from a single exponential decay. The nature of the relaxation processes was investigated through the dependence of the mean relaxation rates Γ on the squared amplitude of the scattering vector, q^2, where the mean values of Γ have been calculated from the distributions given by CONTIN algorithm. The mean relaxation rates corresponding to the individual peaks of the size distribution exhibit a linear dependence on q^2, and the linear fits to the data pass through the origin (Figure 5), indicating that both of the relaxation modes arise from translational diffusion.[37]

The slope of the linear fit representing the diffusion coefficient, $\Gamma/q^2 = D_\theta$, has been used to calculate the hydrodynamic radii corresponding to both relaxation processes. The hydrodynamic radii have been obtained from the Stokes−Einstein relation

$$D = \frac{kT}{6\pi\eta R_h} \tag{4}$$

in which η is the viscosity of the medium and R_h is the hydrodynamic radius. There was only minor variation without any trend in the hydrodynamic radii of the amphiphiles at 90° scattering angle upon increasing ionic strength although it was accompanied by an increase in the scattering intensity prior to the precipitation. The average values of R_h in aqueous NaCl were 19 and 20 nm for the fast mode (Table 2), and 183 and 247 nm for the slow mode of polymers **1** and **2**, respectively. The corresponding values for the sample of polymer **1** with a higher degree of hydrolysis gave values 19 and 225 nm, the latter being within the error of the R_h of the slow mode. The cryoTEM images of the samples at pH 4.90 ($\alpha \sim 0.13$) show that they mainly consist of spherical species with average radii R_{tot} of 17 nm (**1**) and 18 nm (**2**). Some representative micrographs of the polymer solutions are shown in Figure 6. The radius of the sphere R_{tot} has been calculated from the micrographs by $R_{tot} = R_c + R_s$, where R_c is the radius of dark core and R_s is the radius of shell, calculated from the distance between the centers of cores presuming close packing of the micelles. Because the diffusion coefficients $D_\theta = \Gamma/q^2$ of both fast and slow modes showed no angular dependence, being typical for monodisperse spherical species (presented in the Supporting Information), and the radii given by DLS and cryoTEM were the same within the experimental error, we may conclude that the fast mode originates from the spherical aggregates. The cryoTEM micrographs of the samples also reveal the presence of a small fraction of large clusters with irregular shapes (Figure 7), which appear to be the origin of the slow diffusion mode. The presence of large clusters or aggregates is often characteristic for block copolymer samples prepared by direct dissolution method: the dissolution of polymer occurs by slow fragmentation of powder into smaller parts.[39] In the case of the amphiphilic stars, the clusters did not break up during 1 week's dissolution or upon raising the pH to 9.20. Due to the glassy PMMA core, nonequilibrium structures can be formed. Another explanation for the presence of large aggregates could be the aggregation of micelles upon screening of the charges in the polyelectrolyte outer blocks by added salt. Although some larger aggregates could be observed in salt-free solutions, their fraction was indeed higher in the presence of salt, which is in accordance with the computer simulations described below. The methods of the sample preparation need to be studied further.

Zimm plots obtained for the polymer concentrations 0.4−1.0 g/L at scattering angles 40−150° were all nonlinear, thus demonstrating the polydispersity of the studied samples. This is in line with the DLS results showing bimodal size distributions. The Zimm analysis of the SLS data for polymer **2** was performed using the second order polynomial fit. The apparent M_w obtained at zero angle and zero concentration was 24.0×10^6 g/mol (using $dn/dc = 0.157$ mL/g[11]), which most likely represents the large clusters. Strong angular dependence of the intensity of scattered light cannot be expected for small scatterers with R_g close to $\lambda/20$. Molar mass of the smaller species was estimated using large angles. At the range of scattering angles 110−150°, the Zimm method gave the apparent $M_w = 4.6 \times 10^6$ g/mol which can be taken as a rough estimate for the smaller scattering species. However, because the presence of large particles impedes determining the molar masses of smaller species reliably by SLS, the aggregation numbers N_{agg} for the spherical aggregates have been calculated using the results from cryoTEM.

The maximum dimensions of single stars have been estimated from the contour lengths of the arms (Table 2). The minimum radius of the core, R_c(min), can also be calculated by eq 5, assuming the space-filling condition.

$$\frac{4}{3}\pi R_c^3 = N_{agg} N_{MMA} \nu_0 \tag{5}$$

in which N_{MMA} is the amount of MMA units in one block and ν_0 is the molar volume of one MMA unit.[8] The resulting values of R_c(min) were 1.10 nm (**1**) and 1.07 nm (**2**). The hydrodynamic radii were determined also for the $(PMMA)_8$ and $(PMMA\text{-}b\text{-}PtBA)_8$ precursors in a good solvent, THF, being 6.5 and 13.8 nm for polymer **1** and 6.0 and 14.8 nm for polymer **2**, respectively. The aggregation numbers N_{agg} of the spherical aggregates have been calculated using the R_c given by cryoTEM. The values of N_{agg} obtained by eq 5 corresponding to the aggregation number of individual arms (N_{agg}(arm)) have been divided by the number of arms, f. The amphiphile with a longer hydrophilic block gave lower aggregation number: the average values of N_{agg} for the eight-armed stars were 13 and 11 for the polymers **1** and **2**, respectively (Table 2). We would like to apply the model by Förster et al.[40] for amphiphilic block copolymers in order to calculate the theoretical aggregation number of the stars, N_{agg}(theor). According to this model, the aggregation number is dependent on the lengths of both hydrophobic and hydrophilic blocks, and is given by

$$N_{agg} = Z_0 N_A^2 N_B^{-0.8} \tag{6}$$

in which N_A is the length of hydrophobic block and N_B is the length of hydrophilic block. Here the hydrophobic block would have stronger effect on the N_{agg} than the hydrophilic one. Z_0 is the local packing parameter at the core/corona interface, being 0.9 for linear block copolymers of PMMA and PAA.[41] This value of Z_0 gives N_{agg}(theor) = 19 and 11 for the amphiphilic stars **1** and **2**, respectively. Although the theoretical aggregation number of polymer **1** was higher than the experimental one,

Table 2. Properties of the Spherical Micelles from the CryoTEM and Light Scattering Results

entry	solution	R_c(max, theor)[a], nm	R_s(max, theor)[b], nm	R_c, nm	R_s, nm	R_s/R_s (max)[c]	R_s/R_c	N_{agg}[d]	R_{tot}, nm	R_h(DLS)[e], nm	R_g/R_h[e]
1	no salt, pH 4.9	19.2	21.5	6.5 ± 0.8	12.1 ± 4.2	0.56	1.9	13 ± 5	18.6 ± 5.0		
	0.1 M NaCl, pH 4.9			6.4 ± 0.7	10.5 ± 2.6	0.49	1.6	13 ± 4	16.9 ± 3.3	19.4 ± 1.3	0.73
	0.1 M NaCl, pH 12.5			6.2 ± 0.7	20.0 ± 2.4	0.93	3.2	12 ± 4	26.2 ± 3.1	19.4 ± 0.3	0.69
2	no salt, pH 4.9	16.1	27.1	5.7 ± 0.8	16.3 ± 3.0	0.60	2.9	10 ± 6	22.0 ± 3.8		
	0.1 M NaCl, pH 4.9			5.7 ± 0.6	11.7 ± 2.2	0.43	2.0	12 ± 5	17.6 ± 2.8	20.7 ± 1.3	0.63
	0.1 M NaCl, pH 11.9			5.8 ± 0.6	22.9 ± 2.1	0.85	3.9	11 ± 5	28.7 ± 2.7	19.9 ± 0.9	0.54

[a] Theoretical maximum radius of the core given by the contour length of the hydrophobic PMMA block in a single arm, calculated from the repeating units. [b] Theoretical maximum radius of the shell given by the contour length of the hydrophilic PAA block in a single arm, calculated from the repeating units. [c] R_s/R_s(max, theor), describes the stretching of PAA blocks. [d] Calculated from the following equation: $(4\pi R_c^3)/3 = N_{agg}$ (arm) $\times N_{MMA} \times \nu_0$, in which N_{MMA} is the amount of MMA units in one block, N_{agg} (arm) is the number of blocks in the micellar core, and ν_0 is the molar volume of MMA unit. N_{agg} has been obtained by dividing N_{agg} (arm) by the number of arms, f ($f = 8$). [e] Calculated as average values from the measurements at pH 5.1 and pH 9.2, respectively.

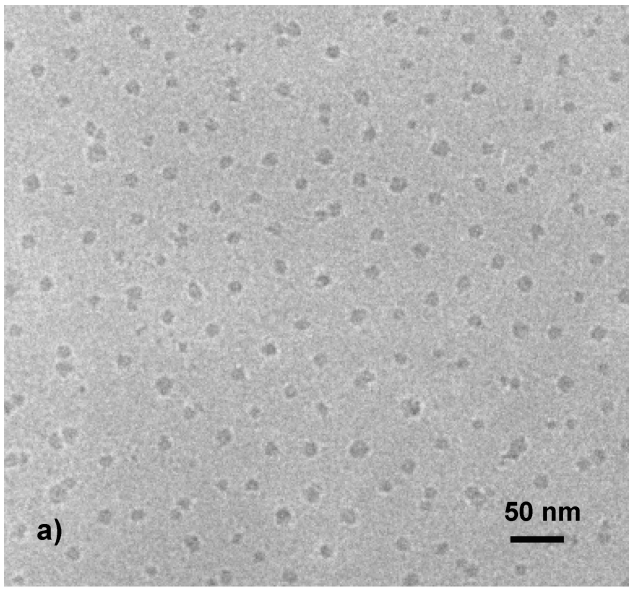

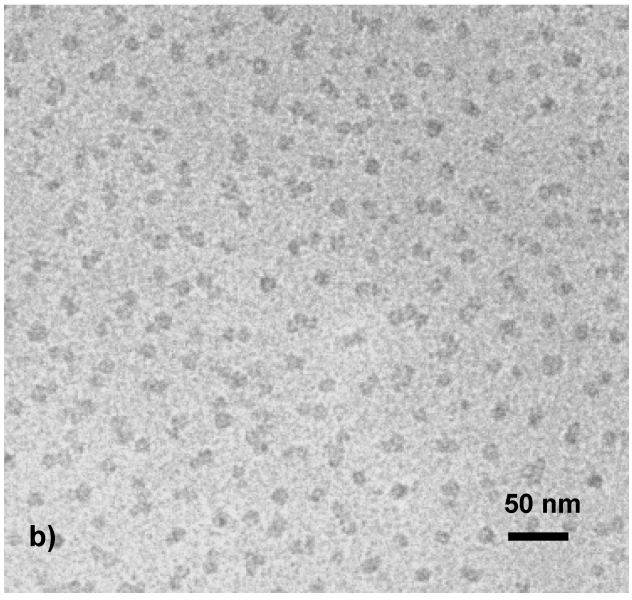

Figure 6. Representative cryoTEM micrographs of aqueous 5.0 g/L solutions of polymer **2** at pH 4.90 (a) in the absence of salt (underfocus 7.6 μm) and (b) in 0.1 M NaCl (underfocus 7.7 μm).

the results are in reasonable agreement with the values calculated from cryoTEM images, suggesting that the same model would apply also to starlike block copolymers, as has earlier been proposed by Burguière at al.[8] for three-arm stars. As polymer **1** exhibited a higher tendency to aggregate than **2** owing to its higher hydrophobic/hydrophilic ratio, it was chosen as a model polymer for the computer simulations when investigating the aggregation behavior of the stars. The simulations and their results are described below.

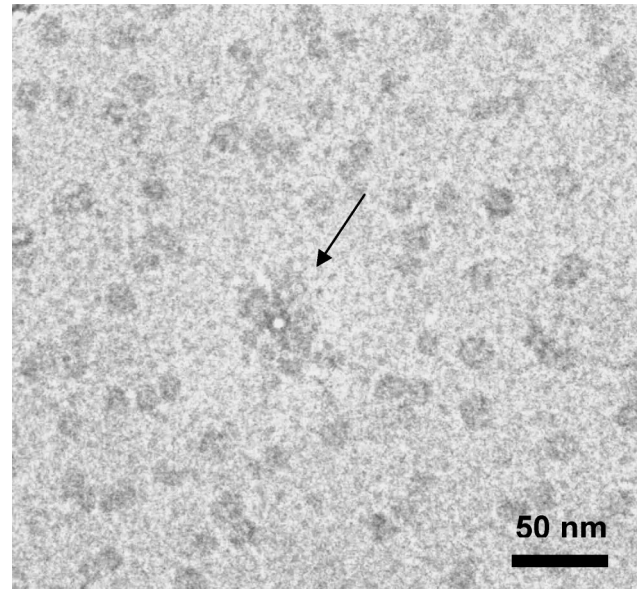

Figure 7. A representative cryoTEM micrograph (underfocus 7.7 μm) of an aqueous 5.0 g/L solution of polymer **2** at pH 4.90 in 0.1 M NaCl showing a large aggregate pointed by a black arrow.

Scheme 2. Layout of the Course-Grained Model of an Eight-Arm Star with Counterions

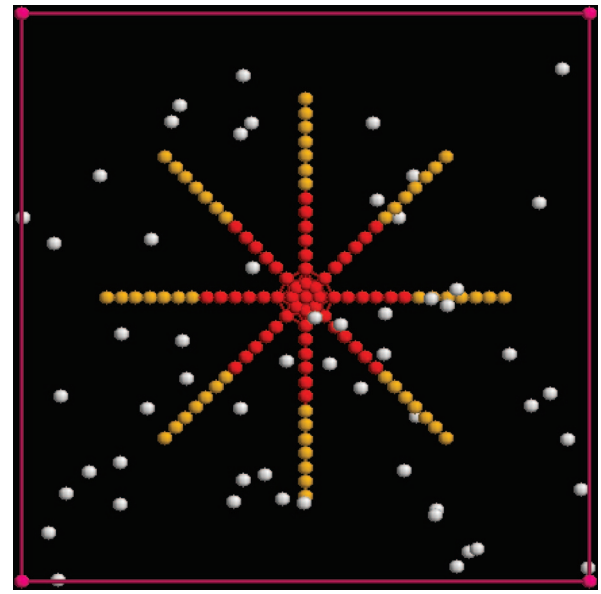

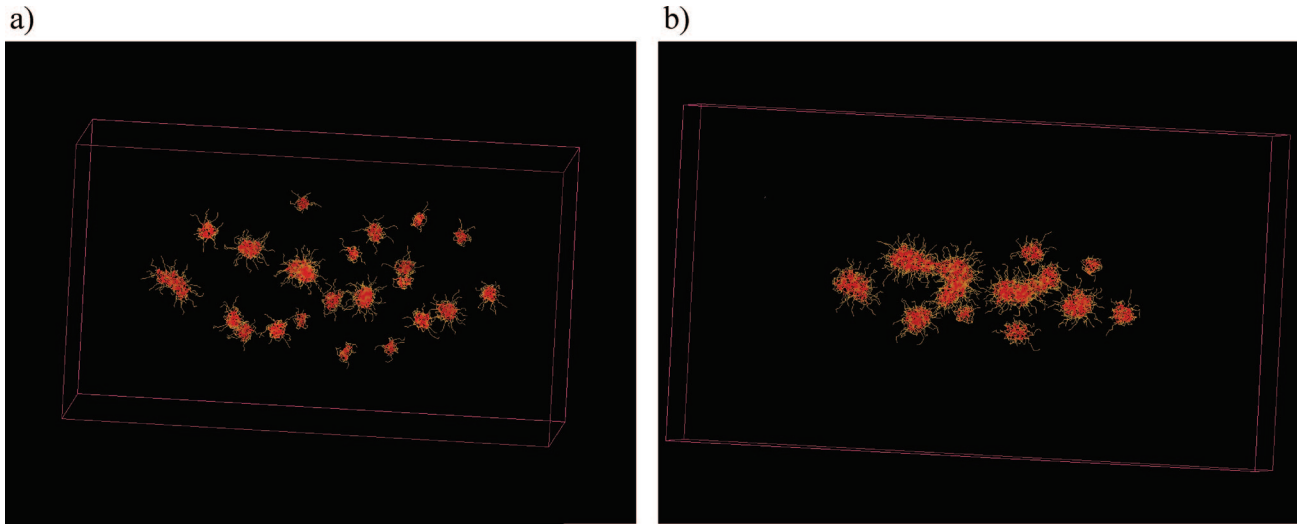

Figure 8. Snapshots of simulated eight-arm star system in a salt free solution (a) and at the presence of salt (rd = 1.5) (b). Counterions are not shown.

The thickness of the polyelectrolyte shell of micelles, R_s, decreased when charges were screened upon the addition of salt at low pH (pH 4.90). When the pH of the solution was increased, PAA blocks became highly stretched up to ~90% of their contour length (Table 2), despite the presence of salt. Stretching of the polyelectrolyte blocks was also reflected by lower R_g/R_h ratios at higher pH. The values of R_g for the micelles were determined from the dependence of the reciprocal time-averaged intensities of fast relaxation process on the squared amplitude of the scattering vector, q^2. The values of R_g/R_h were lower than the hard-sphere limit 0.78 due to the soft corona surrounding the hard core of the micelles,[42,43] being closer to this limit for polymer **1** with shorter hydrophilic blocks. Therefore, higher time-averaged light scattering intensities of the fast relaxation process, $I_f(q)$, for all the solutions of polymer **1** originate from both the larger hydrophobic core and higher average density of the micelles.

Simulations. The spherical micelles observed in the case of eight-arm stars may be more complicated in structure than those in the case of four-arm stars studied previously.[12] Increasing the number of arms may pose constraints to the formation of clear core−shell structures. As has been clearly shown above, the increased number of arms does not prevent the formation of spherical but that of cylindrical micelles and thus, we tested the same model as in the earlier, more simple case. In our previous work,[12] the aggregation behavior of a four-arm $(PMMA_{73}\text{-}b\text{-}PAA_{143})_4$ star block copolymer in aqueous solutions was simulated using a coarse-grained model, which has also been applied here to describe the effect of added salt on the self-assembly of an eight-arm amphiphilic block copolymer resembling polymer **1**, $(PMMA_{77}\text{-}b\text{-}PAA_{86})_8$. In this model, the stars consist of eight flexible diblock copolymer arms with hydrophobic noncharged inner blocks and hydrophilic charged outer blocks. The arms emanate from a common center and are composed of N1 hydrophobic noncharged beads and N2 hydrophilic and negatively charged beads (Scheme 2). As it has been assumed that every bead represents about 10 monomer units of PMMA or PAA, the simulated stars have N1 = N2 = 7. The arms have one common bead, identical to a hydrophobic PMMA bead. To keep the neutrality of the solution, the simulation box also contains small positively charged counterions N3, whose number is equal to the total number of charges in the box. The simulation method and the chosen parameters have been described in more detail in the previous paper.[12] Extending the simulation into the case of eight-arm star helps in evaluating the applicability of the chosen method. In addition, an interesting insight on the chain conformations may be obtained.

In the current work, two systems corresponding to salt-free and saline solutions with the polymer concentration 5.0 g/L have been considered. In the latter case, the concentration of the monovalent salt is 0.1 M, corresponding to the Debye radius $r_D \sim 10$ Å, or 1.5 in sigma units. The simulation box contained 50 eight-arm stars with 113 beads per star. The total number of polymer beads was $N = 5650$. When every bead represents 10 monomer units, the corresponding number density of the polymer ρ is $\rho = N/V = 0.005$. The value of volume V of the simulation box was taken to prepare the model solution with the same number density of the polymer. The number of counterions (with $q = +1$) was 2800, equal to the number of charged polymer beads. In the initial state the system is fully disordered. The equilibration of the system was carried out using a NVT ensemble during 5×10^5 steps. The system was considered as equilibrated when the aggregation number distribution of micelles did not change appreciably during sufficiently long time. Following the equilibration phase, a production run of 5×10^5 time steps was performed and the structural characteristics of the systems were determined.

In all cases, the formation of micelles was observed. The snapshots illustrating the morphology of micellar aggregates obtained under different conditions are shown in Figure 8. It is seen that spherical aggregates are formed both in the salt-free solution (Figure 8a) and in the presence of salt (Figure 8b). The micelles contain a dense core where the chains are collapsed and a loose corona with stretched chains. In the salt-free case the distribution of the aggregation numbers is quite narrow and the average aggregation number is equal to 2.5. The addition of salt increases the aggregation number up to 4.5 but does not change the shape of micelles (Figure 8b). The distribution of aggregation numbers is wider compared to the case of 4-arm stars with the same arm structure.

It is interesting to compare the conformations of the blocks in the micelles. In a salt-free system the mean squared end-to-end distance of the hydrophobic (H) blocks $<h_H^2>^{0.5} = 3.58$ and the hydrophilic (P) blocks $<h_P^2>^{0.5} = 4.65$. The corresponding degrees of stretching are $<h_H^2>^{0.5}/L = 0.44$ and $<h_P^2>^{0.5}/L = 0.66$, respectively, where L is the contour length of a block. To compare the conformation of chains in the core and the corona with those of free chains we have simulated a number of single linear homopolymer chains composed of seven

hydrophobic and seven hydrophilic beads and calculated their unperturbed mean-squared end-to-end distances in the globular $<h_{H,single}^2>$ and swollen $<h_{P,single}^2>$ states, correspondingly. The ratio of $<h_H^2>^{0.5}/<h_{H,single}^2>^{0.5} = 1.9$, and $<h_P^2>^{0.5}/<h_{P,single}^2>^{0.5} = 1.3$. It is seen that the hydrophobic block in the star core is stretched as compared to the conformation of a single chain in the monomolecular globule. The reason for this stretching is the fact that the end of the hydrophobic block should be on the core surface. In the salt-containing regime the chains both in the core and in the corona are less stretched: $<h_H^2>^{0.5}/L = 0.40$ and $<h_P^2>^{0.5}/L = 0.57$, respectively.

The main result of the present simulation is that the spherical morphology remains even if the electrostatic interactions are significantly screened due to the addition of salt. To reveal which factors are responsible for the stability of the spherical morphology we also simulated the solution of four-arm stars with the same arm structure. The concentration of the solution was the same as that of the eight-arm stars. In the salt-free solution these stars formed spherical micelles with an average aggregation number of 5, but in the presence of salt, the formation of wormlike structures took place (see Supporting Information). Unfortunately, we have no experimental data for four-arm stars with such ratio of block lengths. However, in our previous paper it was shown both experimentally and by computer simulation that for four-arm stars with the ratio of block lengths 1:2 a wormlike morphology of aggregates was observed. It is well-known that the decrease of the length of the hydrophilic block favors the cylindrical morphology.[44] Therefore, this morphology would be even more favorable for stars with the ratio of block lengths 1:1. Hence, we may conclude that the large number of arms is the main factor preventing the formation of wormlike micelles for eight-arm stars.

When comparing our results with the experimental data we have taken into account that in our simulation model all the beads of the outer blocks are charged. This case corresponds to the degree of charging of PAA block at high pH > 12 (see our previous work[12]). Simulation predicts a spherical morphology of micelles both for salt-free and salt-containing regime but in the first case the micelles are smaller. The size of the micelles at high pH has been estimated experimentally only in the presence of salt (Table 2, polymer **1**). As the cryoTEM images of the saline polymer solutions with high pH showed a grainlike texture suggesting the disintegration of the micelles and possibly also of the star polymers themselves, salt-free solutions with high pH were not investigated experimentally. However, the aggregates are expected to be spherical also in this case. Therefore, we may conclude that the results of our simulations are in qualitative agreement with the experimental results.

Conclusions

The factors governing the micellar morphologies of amphiphilic block copolymers depend on the surface energy between the core and the solvent, as well as on the stretching of the blocks in the core and the corona of the micelles.[45] According to the experimental observations, eight-arm amphiphilic star block copolymers prefer the spherical morphology of the aggregates above the cac. Unlike in the case of sterically less crowded four-arm amphiphilic stars, which formed cylindrical aggregates in salt solutions,[11,12] adding salt and thus screening the charges in the polyelectrolyte blocks of the eight-arm stars did not induce any morphological transition. The high number of arms results in higher stretching of the core-forming blocks as well as in higher repulsion between the polyelectrolyte blocks in the corona, leading to a lower degree of aggregation. Larger clusters also present in the solutions of eight-arm stars probably stem from the incomplete fragmentation of the polymer during the dissolution, except when larger organic divalent counterions have bridged the polyelectrolyte groups between the aggregates. The cac and the aggregation number were also dependent on the ratio of the lengths of the hydrophobic and hydrophilic blocks, and the aggregation number followed the same scaling relationship as for linear block copolymers. The computer simulations of eight-arm and four-arm stars with corresponding compositions both in the absence and in the presence of salt have also demonstrated that the shape of the stars has a strong influence on the morphology of their aggregates.

Acknowledgment. The work has been done in the frame of an ESF project STIPOMAT. S.S. wishes to thank the Finnish National Graduate School in Nanoscience (NGS-NANO) for financial support. Financial support from the Academy of Finland (project 11464) is acknowledged. A.A.D. is grateful to the RFBR (Grant 05-03-32450) and to Magnus Ehrnrooth fund for financial support. The authors wish to thank Prof. Pavel Khalatur for providing the computer code, Dr. Vladimir Aseyev for helpful discussions, and the Electron Microscopy Unit, Institute of Biotechnology, University of Helsinki, for the Electron Microscopy facilities.

Supporting Information Available: ^{1}H NMR spectra of the synthesized polymers, fluorescence emission spectra and light scattering intensities for the determination of cac, the results of the potentiometric titrations, LS results as well as additional simulation results have been provided. This material is available free of charge via the Internet at http://pubs.acs.org.

References and Notes

(1) Rodríguez-Hernández, J.; Chécot, F.; Gnanou, Y.; Lecommandoux, S. *Prog. Polym. Sci.* **2005**, *30*, 691–724.
(2) Discher, D. E.; Ahmed, F. *Annu. Rev. Biomed. Eng.* **2006**, *8*, 323–341.
(3) Discher, D. E.; Eisenberg, A. *Science* **2002**, *297*, 967–973.
(4) Zhang, L.; Eisenberg, A. *Macromolecules* **1999**, *32*, 2239–2249.
(5) Cui, H.; Chen, Z.; Wooley, K. L.; Pochan, D. J. *Macromolecules* **2006**, *39*, 6599–6607.
(6) Gitsov, I.; Fréchet, J. M. J. *J. Am. Chem. Soc.* **1996**, *118*, 3785–3786.
(7) Yoo, M.; Heise, A.; Hedrick, J. L.; Miller, R. D.; Frank, C. W. *Macromolecules* **2003**, *36*, 268–271.
(8) Burguière, C.; Chassenieux, C.; Charleux, B. *Polymer* **2003**, *44*, 509–518.
(9) Kim, K. H.; Cui, G. H.; Lim, H. J.; Huh, J.; Ahn, C. H.; Jo, W. H. *Macromol. Chem. Phys.* **2004**, *205*, 1684–1692.
(10) Whittaker, M. R.; Monteiro, M. J. *Langmuir* **2006**, *22*, 9746–9752.
(11) Strandman, S.; Hietala, H.; Aseyev, V.; Koli, B.; Butcher, S. J.; Tenhu, H. *Polymer* **2006**, *47*, 6524–6535.
(12) Strandman, S.; Zarembo, A.; Darinskii, A. A.; Löflund, B.; Butcher, S. J.; Tenhu, H. *Polymer* **2007**, *48*, 7008–7016.
(13) Li, Z.; Kesselman, E.; Talmon, Y.; Hillmyer, M. A.; Lodge, T. P. *Science* **2004**, *306*, 98–101.
(14) Xu, J.; Zubarev, E. R. *Angew. Chem., Int. Ed.* **2004**, *43*, 5491–5496.
(15) Tang, J. X.; Janmey, P. A. *J. Biol. Chem.* **1996**, *271*, 8556–8563.
(16) Huh, J.; Kim, K. H.; Ahn, C.-H.; Jo, W. H. *J. Chem. Phys.* **2004**, *121*, 4998–5004.
(17) Sheng, Y.-J.; Nung, C.-H.; Tsao, H.-K. *J. Phys. Chem. B* **2006**, *110*, 21643–21650.
(18) Nikitine, S.; Heimburger, R.; Ringeissen, J.; Schwab, C. Pat. Appl. FR 1523459, **1968**.
(19) Strandman, S.; Tenhu, H. *Polymer* **2007**, *48*, 3938–3951.
(20) McLaughlin, A.; Eng, W.-K.; Vaio, G.; Wilson, T.; McLaughlin, S. *J. Membr. Biol.* **1983**, *76*, 183–193.
(21) Strandman, S.; Pulkkinen, P.; Tenhu, H. *J. Polym. Sci., Part A: Polym. Chem.* **2005**, *43*, 3349–3358.
(22) Ma, Q.; Wooley, K. *J. Polym. Sci., Part A: Polym. Chem.* **2000**, *38*, 4805–4820.
(23) Klucker, R.; Munch, J. P.; Schosseler, F. *Macromolecules* **1997**, *30*, 3839–3848.
(24) Adrian, M.; Dubochet, J.; Lepault, J.; McDowall, A. W. *Nature* **1984**, *308*, 32–36.
(25) Colombani, O.; Ruppel, M.; Schubert, F.; Zettl, H.; Pergushov, D. V.; Müller, A. H. E. *Macromolecules* **2007**, *40*, 4338–4350.
(26) Nagasawa, M.; Murase, T.; Kondo, K. *J. Phys. Chem.* **1965**, *69*, 4005–4012.

(27) Taton, D.; Cloutet, E.; Gnanou, Y. *Macromol. Chem. Phys.* **1998**, *199*, 2501–2510.
(28) Yang, Z.; Liu, J.; Huang, Z.; Shi, W. *Eur. Polym. J.* **2007**, *43*, 2298–2307.
(29) Nelson, P. H.; Rutledge, G. C.; Hatton, T. A. *Comp. Theor. Polym. Sci.* **1998**, *8*, 31–38.
(30) Winnik, F. M.; Regismond, S. T. A. *Colloids Surf.* **1996**, *118*, 1–39.
(31) Pal, S. K.; Sukul, D.; Mandal, D.; Sen, S.; Bhattacharyya, K. *Chem. Phys. Lett.* **2000**, *327*, 91–96.
(32) Sen, S.; Dutta, P.; Mukherjee, S.; Bhattacharyya, K. *J. Phys. Chem. B* **2002**, *106*, 7745–7750.
(33) Pal, S. K.; Mandal, D.; Sukul, D.; Sen, S.; Bhattacharyya, K. *J. Phys. Chem. B* **2001**, *105*, 1438–1441.
(34) Virtanen, J.; Lemmetyinen, H.; Tenhu, H. *Polymer* **2001**, *42*, 9487–9493.
(35) Bondarev, S. L.; Knyukshto, V. N.; Stepuro, V. I.; Stupak, A. P.; Turban, A. A. *J. Appl. Spectrosc.* **2004**, *71*, 194–201.
(36) Schillén, K.; Brown, W.; Johnsen, R. M. *Macromolecules* **1994**, *27*, 4825–4832.
(37) Jørgensen, E. B.; Hvidt, S.; Brown, W.; Schillén, K. *Macromolecules* **1997**, *30*, 2355–2364.
(38) Antonietti, M.; Heinz, S.; Schmidt, M.; Rosenauer, C. *Macromolecules* **1994**, *27*, 3276–3281.
(39) Rager, T.; Meyer, W. H.; Wegner, G.; Winnik, M. A. *Macromolecules* **1997**, *30*, 4911–4919.
(40) Förster, S.; Zisenis, M.; Wenz, E.; Antonietti, M. *J. Chem. Phys.* **1996**, *104*, 9956–9970.
(41) Schuch, H.; Kligler, J.; Rossmanith, P.; Frechen, T.; Gerst, M.; Feldthusen, J.; Müller, A. H. E. *Macromolecules* **2000**, *33*, 1734–1740.
(42) Antonietti, M.; Bremser, W.; Schmidt, M. *Macromolecules* **1990**, *23*, 3796–3805.
(43) Qin, A.; Tian, M.; Ramireddy, C.; Webber, S. E.; Munk, P.; Tuzar, Z. *Macromolecules* **1994**, *27*, 120–126.
(44) Borisov, O. V.; Zhulina, E. B. *Macromolecules* **2003**, *36*, 10029–10036.
(45) Halperin, A.; Tirrell, M.; Lodge, T. P. *Adv. Polym. Sci.* **1992**, *100*, 31–71.

MA801475P